Electronic Supplementary Information

A bridged low band gap A-D-A quaterthiophene as efficient donor for organic solar cells

François Baert,[a] Clément Cabanetos,[a] Antoine Leliège,[a] Eva Kirchner,[a] Olivier Segut,[a] Olivier Alévêque,[a] Magali Allain,[a] Gijun Seo,[b] Sungyeop Jung,[b] Denis Tondelier,[b] Bernard Geffroy,[c] Jean Roncali,[a] Philippe Leriche[a] and Philippe Blanchard*[a]

[a] MOLTECH-Anjou, CNRS UMR 6200, University of Angers, Group Linear Conjugated Systems, 2 Bd Lavoisier, 49045 Angers, France. E-mail: philippe.blanchard@univ-angers.fr

[b] LPICM, Ecole Polytechnique, CNRS UMR-7647, 91128 Palaiseau, France

[c] LICSEN, CEA Saclay IRAMIS/NIMBE, 91191 Gif sur Yvette, France

1. Synthesis and NMR spectra.

4,4-Diethyl-4*H*-cyclopenta[2,1-*b*:3,4-*b*’]dithiophene **3** was prepared following the procedure of Vanderzande *et al.*[S1] as described below.

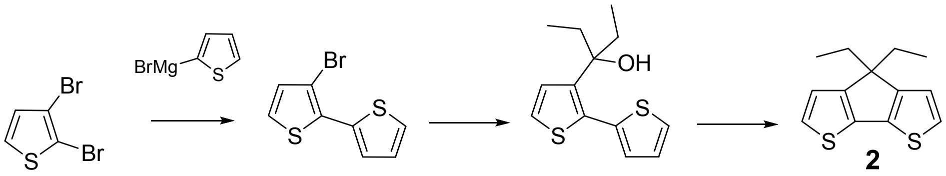

Scheme S1

*3-Bromo-2,2’-bithiophene***.** A Grignard solution was prepared by controlled addition of 2-bromothiophene (7.75 g, 4.60 mL, 47.5 mmol) on magnesium (1.81 g, 74.4 mmol) in anhydrous diethyl ether (60 mL) and further reflux for 45 minutes under argon. This Grignard solution was added dropwise under argon to a stirred and cooled (about 0°C) suspension of $Pd(dppf)Cl_2\cdot CH_2Cl_2$ ([1,1′-Bis(diphenylphosphino)ferrocene]dichloropalladium(II), complex with dichloromethane, 338 mg, 0.41 mmol) and 2,3-dibromothiophene (10 g, 4.68 mL, 41 mmol) in anhydrous diethyl ether (20 mL). After stirring at 0°C for 14h, 20 mL of methanol was added and the mixture was filtered through a 3 cm $MgSO_4$/silica gel double layer. After further washing of the layer with 30 mL of diethyl ether, the combined solutions were rotary evaporated under *vacuum*. The residual oil was purified by column chromatography on silica gel (eluent: petroleum ether) yielding 3-bromo-2,2’-bithiophene

(9.91 g, 40.4 mmol, 98%) as a colorless oil. ^{1}H NMR (300 MHz, $CDCl_3$, δ): 7.42 (dd, *J*=3.7, 1.2, 1H), 7.36 (dd, *J*=5.2, 1.2, 1H), 7.19 (d, *J*=5.4, 1H), 7.09 (dd, *J*=5.2, 3.7, 1H), 7.02 (d, *J*=5.4, 1H) (in accordance with literature[S2]).

3-(2,2'-Bithiophen-3-yl)pentan-3-ol. A solution of 3-bromo-2,2'-bithiophene (9.80 g, 40.0 mmol) in 20 mL anhydrous diethyl ether was added slowly over 15 min to a solution of *n*-BuLi (2.5 M in hexanes, 16.8 mL, 42.0 mmol) in 60 mL anhydrous diethyl ether cooled to -78°C under argon. 3-Pentanone (3.44 g, 4.32 mL, 40.0 mmol) was added *via* a syringe to the mixture at -78°C, followed by stirring at room temperature for 14h. The reaction was quenched at 0°C with a saturated aqueous solution of NH_4Cl. The organic phase was separated and the aqueous phase was extracted with diethyl ether. The combined organic phases were washed with brine, dried with $MgSO_4$ and concentrated under reduced pressure. The oily residue was purified by column chromatography on silica gel (eluent: CH_2Cl_2/petroleum ether 1:3 to CH_2Cl_2) yielding 3-(2,2'-bithiophen-3-yl)pentan-3-ol (8.57 g, 34.0 mmol, 85%) as a slightly yellow oil. ^{1}H NMR (300 MHz, $CDCl_3$, δ): 7.37 (dd, *J*=5.2, 1.0, 1H), 7.26 (d, *J*=5.4, 1H), 7.12 (dd, *J*=3.5, 1.0, 1H), 7.02 (dd, *J*=5.2, 3.5, 1H), 6.97 (d, *J*=5.4, 1H), 1.96 (s, 1H), 1.89 – 1.65 (m, 4H), 0.82 (t, *J*=7.4, 6H) (in accordance with literature [S1]).

4,4-Diethyl-4H-cyclopenta[1,2-b:5,4-b']dithiophene ***3***. H_2SO_4 (27 mL) was added dropwise to 3-(2,2'-bithiophen-3-yl)pentan-3-ol (8.57 g, 34.0 mmol) in 350 mL of *n*-octane under stirring at room temperature. After additional stirring of 20h, the reaction mixture was poured into water and CH_2Cl_2 was added. The organic phase was separated and washed with a saturated $NaHCO_3$ solution, dried with $MgSO_4$ and concentrated under reduced pressure. The crude oil was purified by column chromatography on silica gel (eluent: petroleum ether) yielding **3** (4.16 g, 17.8 mmol, 52%) as a white oil. ^{1}H NMR (300 MHz, $CDCl_3$, δ): 7.16 (d, *J*=4.9, 2H), 6.93 (d, *J*=4.9, 2H), 1.89 (q, *J*=7.4, 4H), 0.59 (t, *J*=7.4, 6H) (in accordance with literature[S1]).

References:

S1 S. Van Mierloo, P. J. Adriaensens, W. Maes, L. Lutsen, T. J. Cleij, E. Botek, B. Champagne, D. J. Vanderzande, *J. Org. Chem.* **2010**, *75*, 7202-7209.

S2 U. Harm, R. Burgler, W. Furbeth, K. M. Mangold, K. Juttner, *Macromol. Symp.* **2002**, *187*, 65-75.

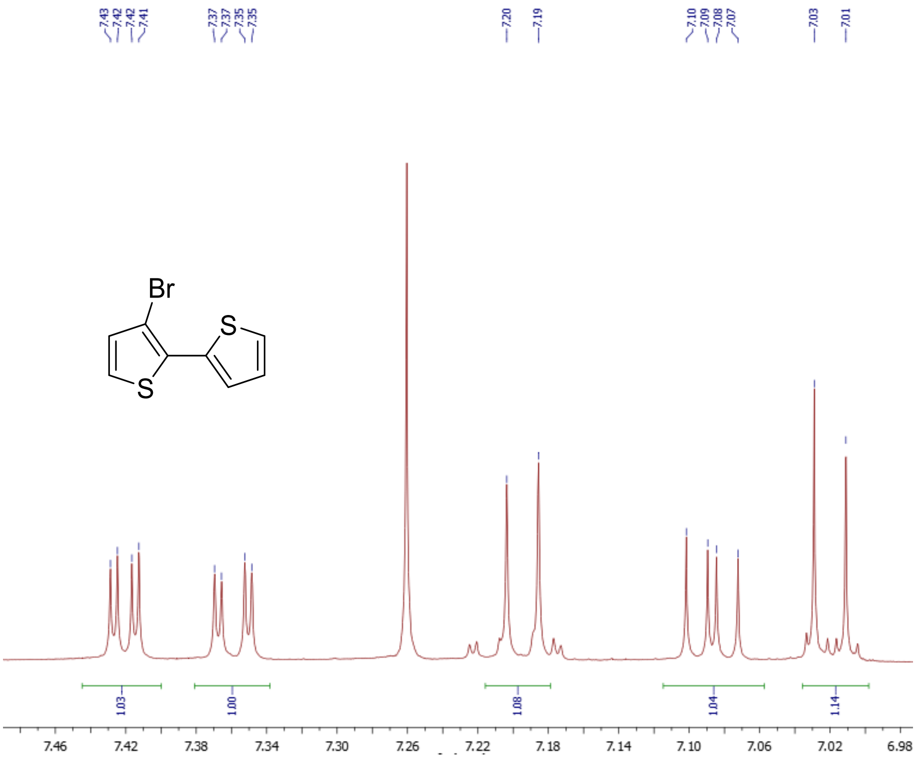

Fig. S1 ^{1}H NMR (300 MHz) spectrum of 3-bromo-2,2'-bithiophene in $CDCl_3$ at 20°C.

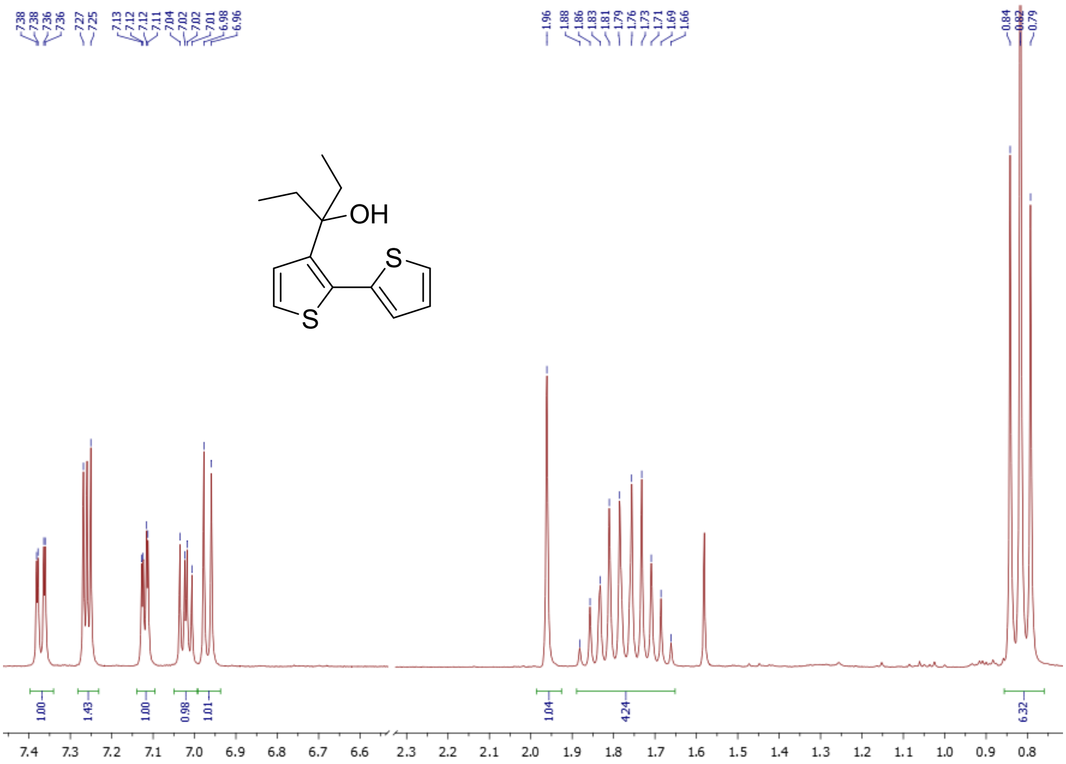

Fig. S2 ^{1}H NMR (300 MHz) spectrum of 3-(2,2'-bithiophen-3-yl)pentan-3-ol in $CDCl_3$ at 20°C.

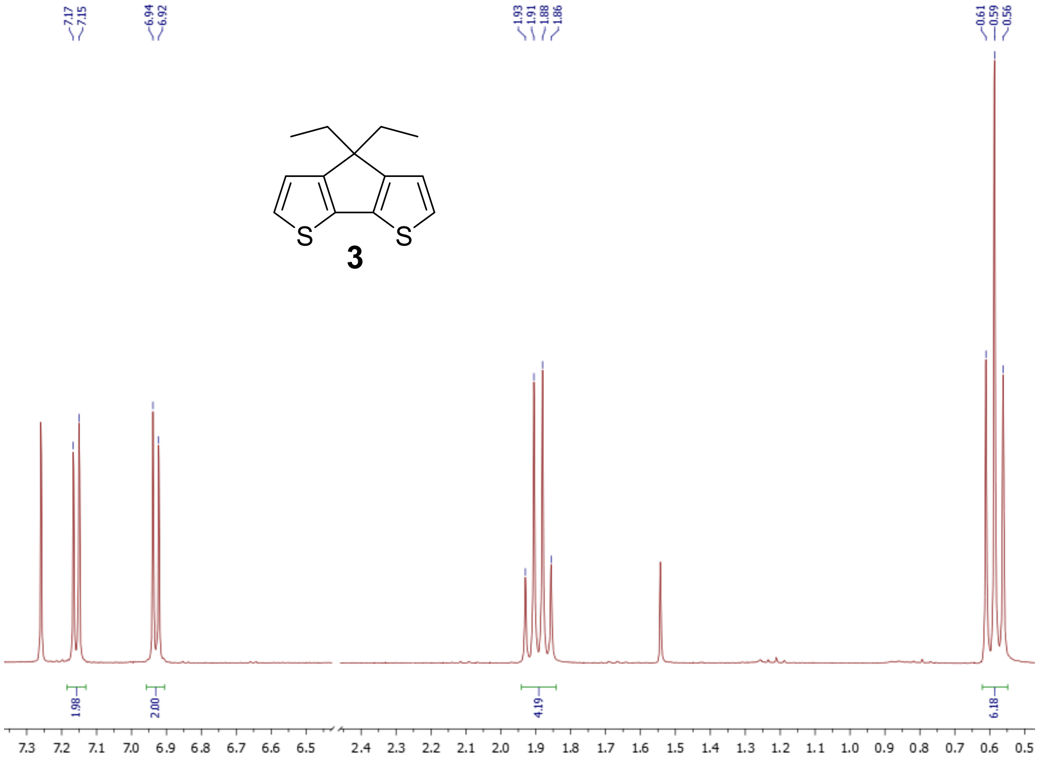

Fig. S3 ^{1}H NMR (300 MHz) spectrum of **3** in $CDCl_3$ at 20°C.

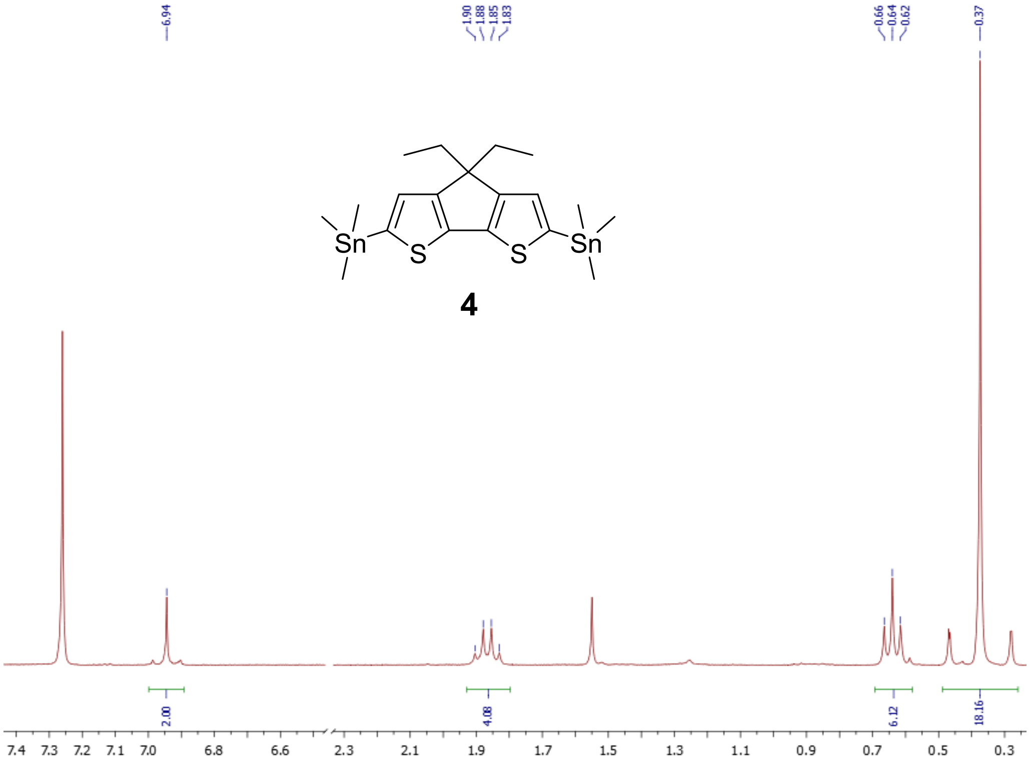

Fig. S4 ^{1}H NMR (300 MHz) spectrum of **4** in $CDCl_3$ at 20°C.

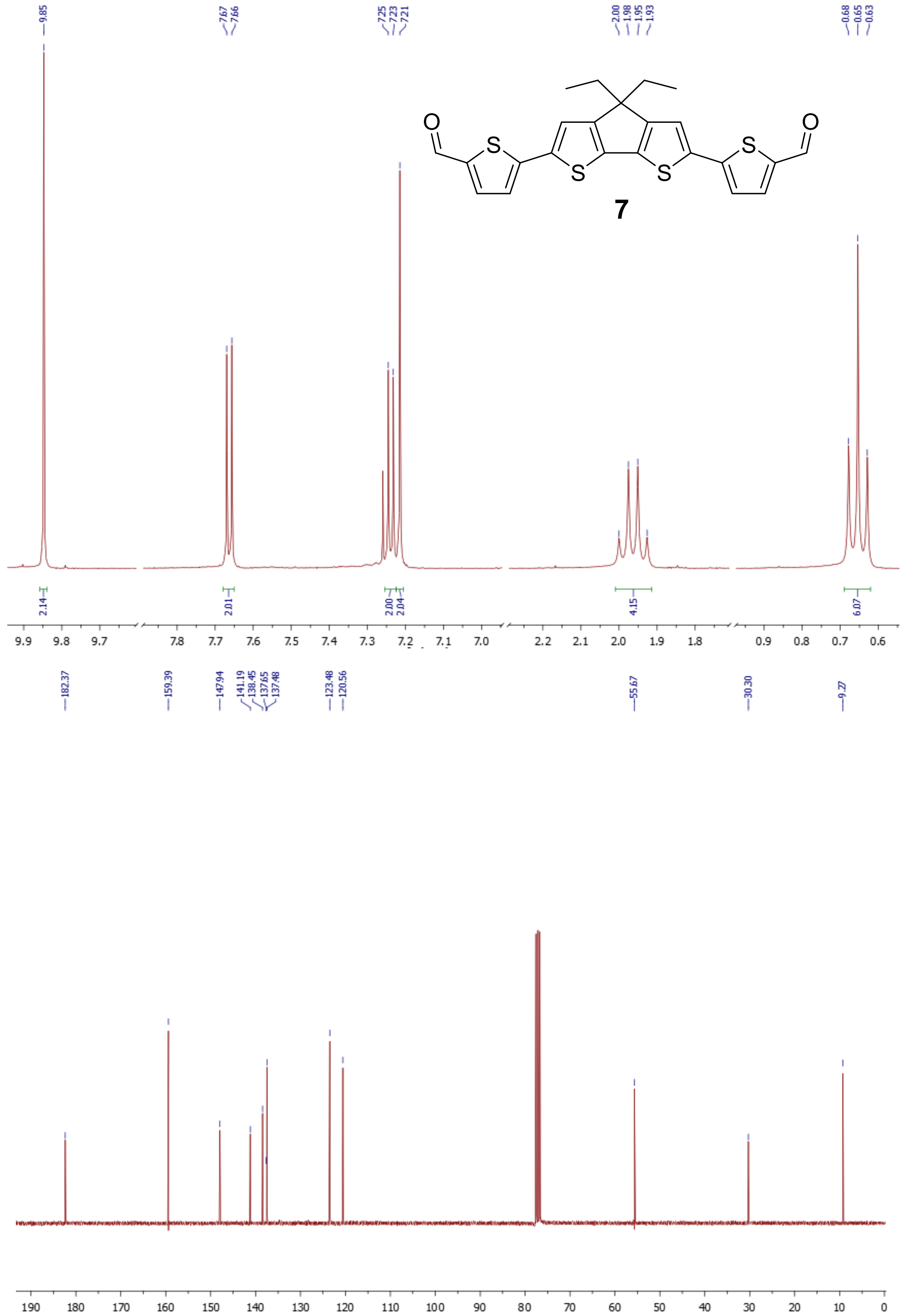

Fig. S5 ^{1}H (300 MHz, top) and ^{13}C (75 MHz, bottom) NMR spectra of **7** in CDCl$_3$ at 20°C.

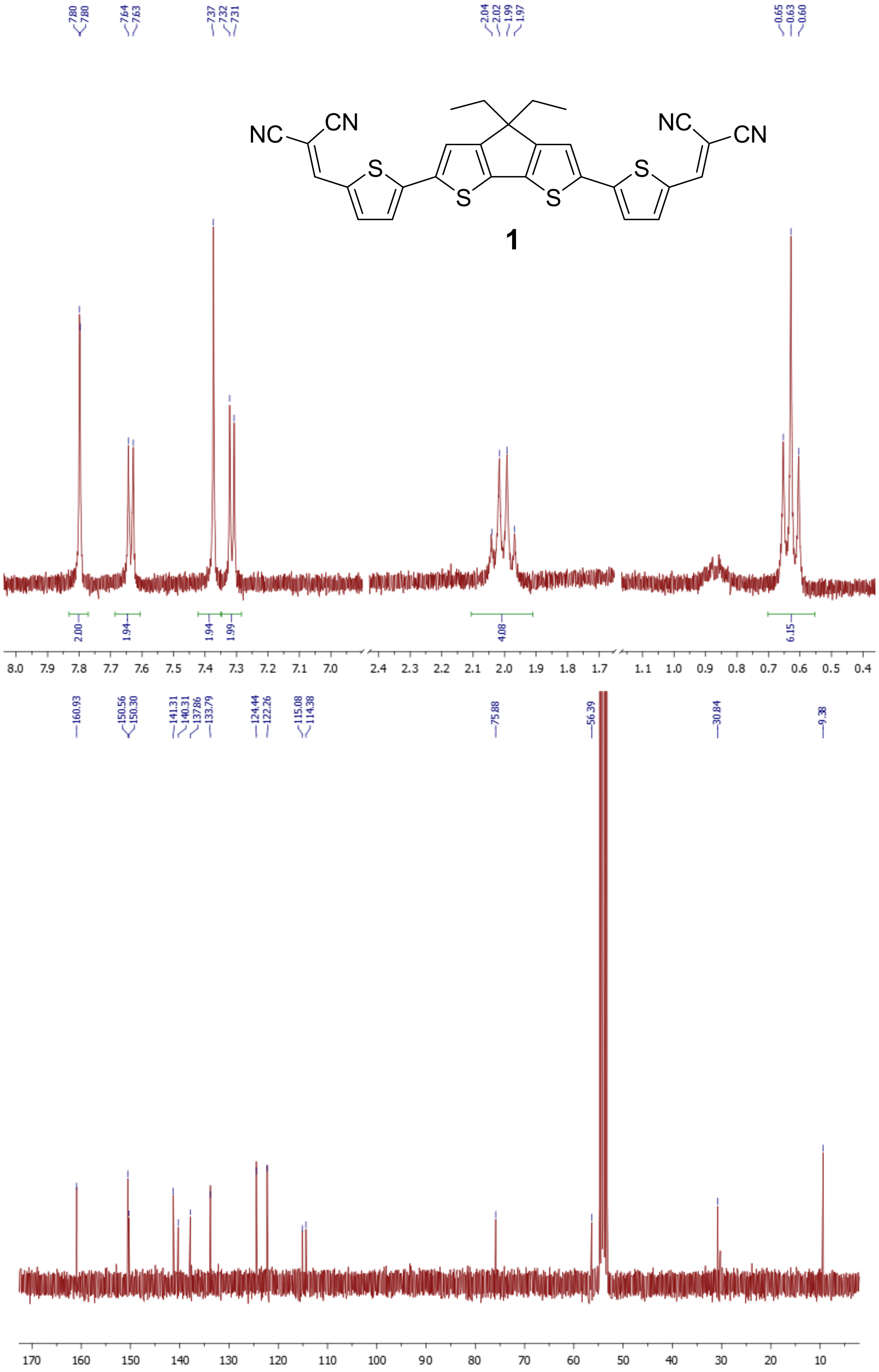

Fig. S6 ^{1}H (300 MHz, top) and ^{13}C (75 MHz, bottom) NMR spectra of **1** in $CDCl_3$ at 20°C.

2. Crystallographic structure of compound 1 (FB086).

X-ray single-crystal diffraction data were collected at 293K on a BRUKER-NONIUS KappaCCD diffractometer, equipped with a graphite monochromator utilizing MoKα radiation (λ = 0.71073Å). The structures were solved by direct methods and refined on F^2 by full-matrix least-squares method, using SHELX-97 package (G.M. Sheldrick, 1998). All non-H atoms were refined anisotropically and the H atoms were included at calculated positions without refinement. Disorder on the chloroform molecule was treated to lead to occupation rate of 1, 0.91, 0.83 and 0.26 for Cl3, Cl1, Cl2 and Cl4 respectively. The Absorption was corrected by SADABS program (Bruker AXS area detector scaling and absorption correction, v2008/1, Sheldrick, G.M. (2008)). CCDC reference numbers 1007813.

Table S1. Crystal data and structure refinement for compound **1**.

Compound	**1**
Empirical formula	$C_{30}H_{19}Cl_3N_4S_4$
Formula weight	670.08
Temperature	293(2) K
Wavelength	0.71073 Å
Crystal system, space group	Triclinic, *P* -1
Unit cell dimensions	a = 7.7895(8) Å b = 11.882(3) Å c = 17.8299(6) Å α = 84.474(9)° β = 78.079(4)° γ = 80.66(2)°
Volume	1589.9(4) $Å^3$
Z, Calculated density	2, 1.400 g/cm^3
Absorption coefficient	0.578 mm^{-1}
Crystal size	0.40 x 0.11 x 0.05 mm
Theta range for data collection	3.21 to 27.56°
Reflections collected / unique	37540/ 7241 [R(int) = 0.0995]
Max. and min. transmission	0.972 and 0.844
Data [I>2sigma(I)] / restraints / parameters	3982 / 1/ 378
Goodness-of-fit on F^2	1.039
Final R indices [I>2sigma(I)]	R1 = 0.0696, wR2 = 0.1551
R indices (all data)	R1 = 0.1666, wR2 = 0.1961
Largest diff. peak and hole	0.569 and -0.570 $e.A^{-3}$

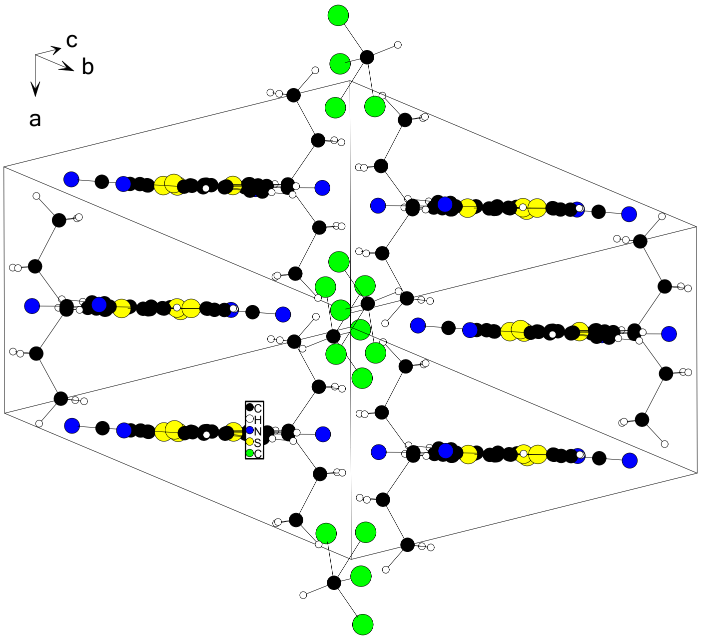

Fig. S7 Molecular packing of molecules **1** along the *a* axis as in the case of Fig. 2 in the presence of $CHCl_3$ molecules.

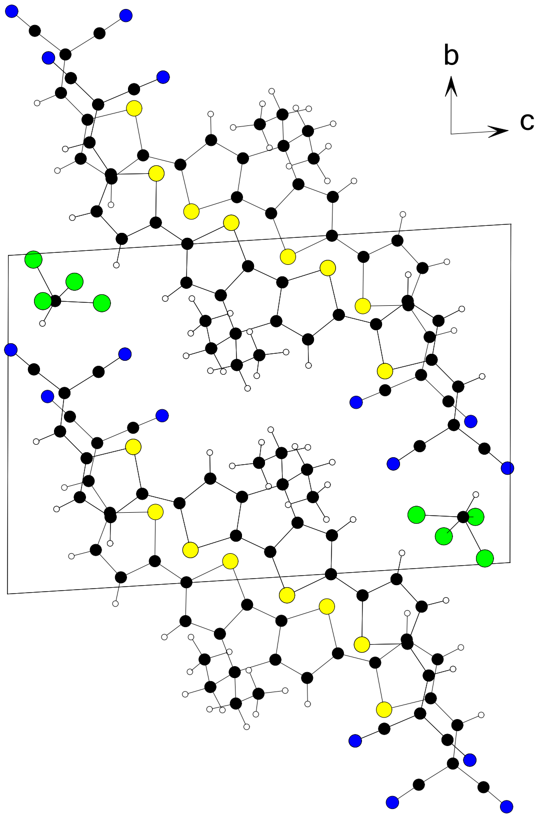

Fig. S8 Overlap of molecules **1** viewed in the *bc* plane as in the case of Fig. 3 in the presence of $CHCl_3$ molecules.

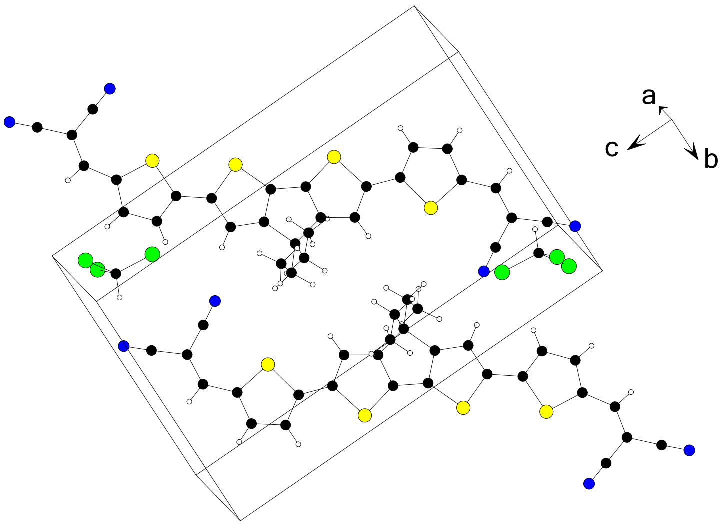

Fig. S9 View showing the possibility of N···H intermolecular contacts as in the case of Fig. 4 even in the presence of $CHCl_3$ molecules.

X-Ray Diffraction (XRD) analysis of thin-films have been performed on a PW1050 Philips diffractometer in Bragg-Brentano geometry using a Cu-Kα radiation ($\lambda = 1.5406$ Å).

3. TGA and DSC analysis.

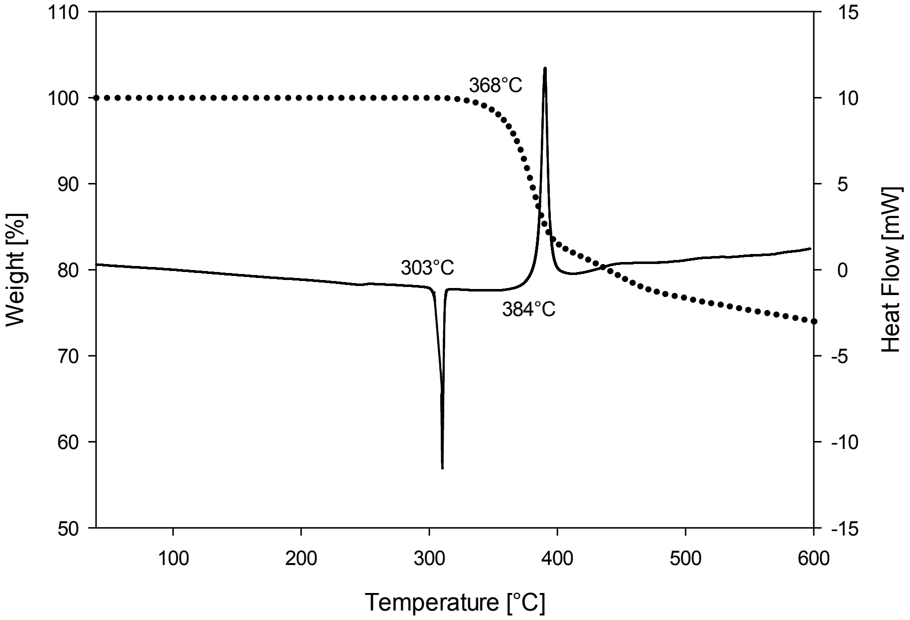

Fig. S10 TGA (dotted line) and first DSC (solid line) traces of compound **1** at a heating rate of 5°C/min under N_2 atmosphere.

4. Cyclic voltammetry of compound 1.

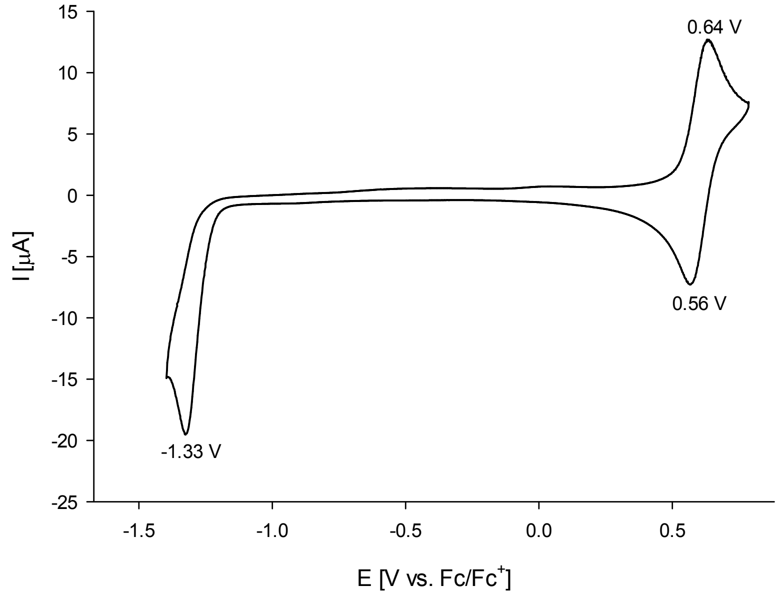

Fig. S11 CV of compound **1** (1 mM) in 0.10 M Bu_4NPF_6/CH_2Cl_2, scan rate 100 mVs^{-1}, Pt working electrode (2 mm diameter).

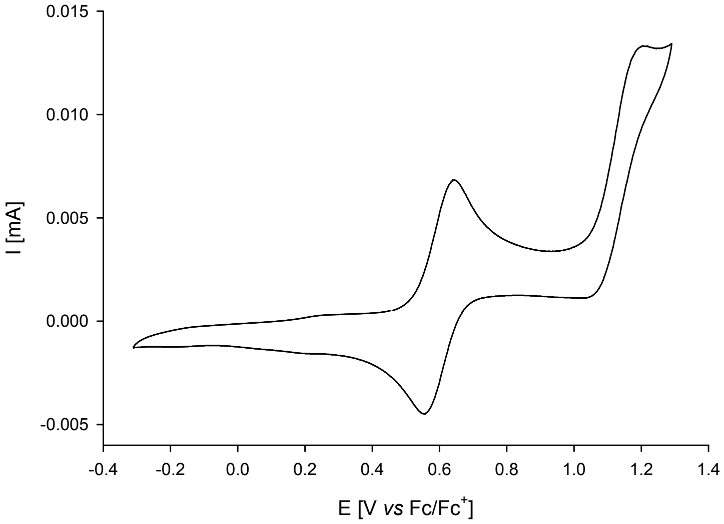

Fig. S12 CV of compound **1** (1 mM) in 0.10 M Bu_4NPF_6/CH_2Cl_2, scan rate 100 mVs^{-1}, Pt working electrode (2 mm diameter).

5. Fabrication of devices.

BL-PHJ solar cells performed at MOLTECH-Anjou. Indium-tin oxide coated glass slides of 24×25×1.1 mm with a surface resistance of 7 Ω/□ were purchased from Praezisions Glas & Optik GmbH. The ITO layer was patterned *via* 37% HCl and Zn etching. The substrates were then washed with Deconex® 12 PA-x solution 2% in water (from VWR international GmbH) and scrubbed using dishwashing soap before being cleaned in ultrasonic, distilled water (15.3 MΩ cm^{-1}), acetone, isopropanol successively for 15 min and dried under a flow of dry nitrogen. A UV-ozone plasma treatment was then performed (UV/Ozone ProCleaner Plus, Bioforce Nanosciences) to increase the hydrophilic nature of the surface and to remove traces of organic compounds for 15 min. Thereafter, electrodes were modified by a spin-cast layer of PEDOT:PSS (Clevios P VP. AI 4083 (HC-Starck) filtered through a 0.45 µm PTFE membrane (Millex®) just prior to use). Spin-casting was achieved with a G3P-8 Spin Coater (Cookson Electronics SCS) at 5000 rpm (ramp = 10 s, t = 60 s), and the electrode was then dried at 140°C for 15 min. Films of donor materials of 10-20 nm thickness were prepared by thermal evaporation under *ca*. 10^{-7} mbar (Plassys Bestek ME300). Finally, 20 nm of C_{60} fullerene (99+%) (MER Corporation) and 150 nm of aluminium were successively and thermally evaporated on top of the donor layer through a mask defining six cells of 0.27 cm^2 area (1.35×0.2 cm^2) on each substrate. Each batch comprised 8 slides. In addition, one mask defining two discoidal cells of 8.0 mm diameter (0.50 cm^2) on each ITO electrode was used for external quantum efficiency (EQE) spectra and also for complementary *J vs V* curves. The thickness of evaporated materials (donor and C_{60}) were monitored by using the oscillating quartz crystal within the evaporator chamber and were afterward confirmed by contact profilometry. Two sets of experiments were performed at differents dates giving reproducible results for both compound **1** or **2**.

The *J vs V* curves of the devices were recorded in a glove box (200B, MBraun) in the dark and under illumination using a Keithley 236 source-measure unit and a home-made acquisition program. The light source is an AM1.5 Solar Constant 575 PV simulator (Steuernagel Lichttecknik, equipped with a metal halogen lamp). The light intensity was measured by a broad-band power meter (13PEM001, Melles Griot) and regularly controlled with an amorphous Si reference cell. The devices were illuminated through the ITO electrode side. EQE was measured under ambient atmosphere using a halogen lamp (Osram) with an Action Spectra Pro 150 monochromator, a lock-in amplifier (Perkin-Elmer 7225) and a S2281 photodiode (Hamamatsu).

Table S2. Photovoltaic parameters of bi-layer donor/C_{60} solar cells under AM 1.5 simulated solar illumination with an average power intensity of *ca.* 80 mW cm^{-2}.[a,b,c]

Entry	Device	Donor thickness (nm)	Cell area (mm^2)	V_{oc} (V)	J_{sc} (mA/cm^2)	*FF*	*PCE* (%)	Device nb	Intensity (mW/cm^2)
1	**1**/C_{60}	10	27	0.83 (0.03) *0.85*	3.75 (0.18) *4.00*	0.43 (0.02) *0.44*	1.66 (0.11) *1.89*	18	79.72
2	**1**/C_{60}	15	27	0.94 (0.02) *0.97*	4.88 (0.36) *5.07*	0.41 (0.02) *0.45*	2.34 (0.18) *2.82*	37	78.30
3	**1**/C_{60}	20	27	0.94 (0.02) *0.95*	3.55 (0.38) *4.19*	0.36 (0.02) *0.39*	1.50 (0.20) *1.92*	25	79.86
4	**2**/C_{60}	15	27	0.86 (0.03) *0.88*	1.50 (0.19) *1.74*	0.24 (0.01) *0.25*	0.41 (0.06) *0.51*	22	75.16
5	**1**/C_{60}[d]	15	50	0.96 (0.02) *0.96*	5.22 (0.43) *5.74*	0.39 (0.03) *0.40*	2.49 (0.28) *2.79*	6	79.20
6	**1**/C_{60} After 100d[e]	15	27	0.98 (0.01) *0.99*	4.79 (0.05) *4.81*	0.36 (0.01) *0.36*	2.14 (0.08) *2.21*	3	78.61

[a] General structure of the bi-layer solar cells ITO/PEDOT:PSS (40 nm)/Donor/C_{60} (20 nm)/Al (150 nm). [b] 0.27 cm^2 area (1.35×0.2 cm^2). [c] Average values, (standard deviation in brakets), *values corresponding to the highest PCE in italics*. [d] 0.50 cm^2 disk area (diameter = 0.8 cm). [e] After 100 days of storage under the light of the day in a glove-box.

In addition, we have examined the PV properties of disk-shaped bi-layer cells based on **1** and displaying an active area of 50 mm^2 (Table S2, entry 5). The photovoltaic parameters remain constant upon increasing the surface area from 27 mm^2 to 50 mm^2 (entries 2 and 5). Besides, first investigations on the long-term stability of the bi-layer solar cells based on **1** (entries 2 and 6) show a *ca.* 10% decrease of the average *PCE* value after 100 days of storage under the light of the day in a glove-box.

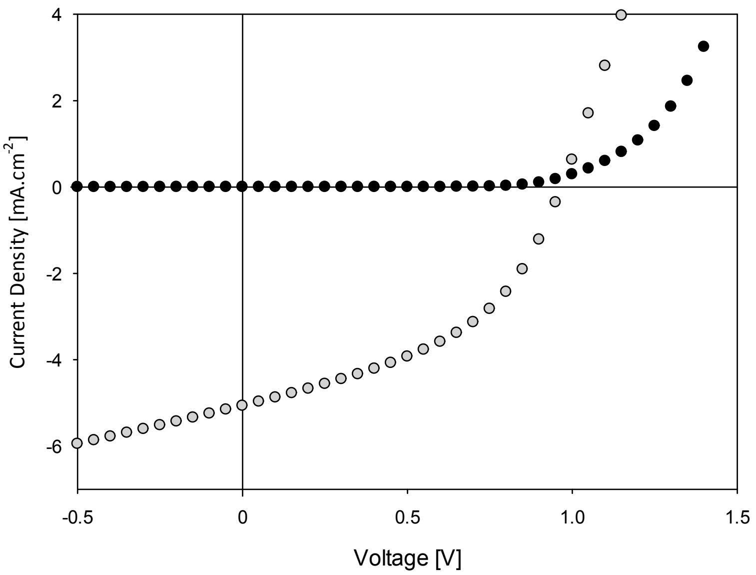

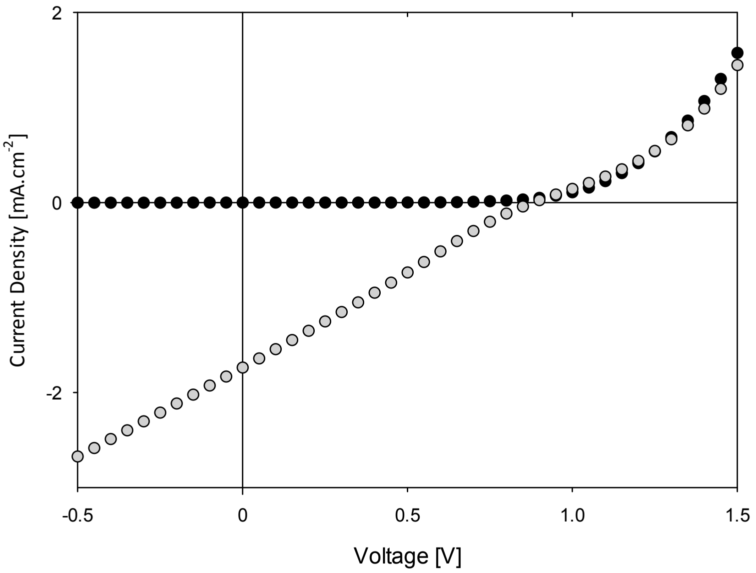

Fig. S13 Plots of current density *vs* voltage of bi-layer PHJ cells ITO/PEDOT-PSS/donor (15 nm)/C_{60} (20 nm)/Al (150 nm) for **1** (top) and **2** (bottom) in the dark (black circles) and under AM 1.5 simulated solar light (80 mW cm^{-2}) (grey circles).

BHJ solar cells performed at LPICM-Polytechnique. Indium-tin oxide coated glass slides of 17×25×1.1 mm with a surface resistance of less than 20 Ω/□ were purchased Xin Yan Technology Ltd. Part of the ITO layer was etched away with 37% HCl and Zn powder. The ITO electrodes were then cleaned in ultrasonic bath successively with 1% of detergent (TFD4) in distilled water, 3 times distilled water, acetone, isopropanol for 15 min each and dried under a flow of dry nitrogen. Finally a UV/O$_3$ treatment is done for 15 minutes. The electrodes were then modified by a spin-cast layer of PEDOT:PSS (Clevios P VP. AI 4083 (HC-Starck) filtered through a 0.45 µm PTFE membrane (Millex®) just prior to use) in a glove box. Then after 30 minutes of annealing at 120°C, the samples were transferred, always under nitrogen, in the thermal evaporator in order to deposit all the layers. Organic materials used in this study have been purchased to Lumtec Technology or Ossila Company. The different organic layers were successively evaporated at a pressure below 4×10^{-7} mbar and the devices were completed by depositing 1.2 nm of lithium fluoride (LiF) and a 100 nm thick aluminum layer as a top electrode through a shadow mask, defining a device area of 0.28 cm^2.

The current density-voltage (J–V) measurements of the fabricated OSCs were performed under the illumination of a simulated AM 1.5G solar light (100 mW cm^{-2}) connected to a computer-controlled Keithley 2635 source measurement unit (SMU) inside a nitrogen-filled glove box. The light source is an AM1.5 Solar Constant 575 PV simulator (ATLAS, equipped with a metal halogen lamp). The light intensity was measured by a broad-band power meter, calibrated (13PEM001, Melles Griot) and regularly controlled with an amorphous Si reference cell.

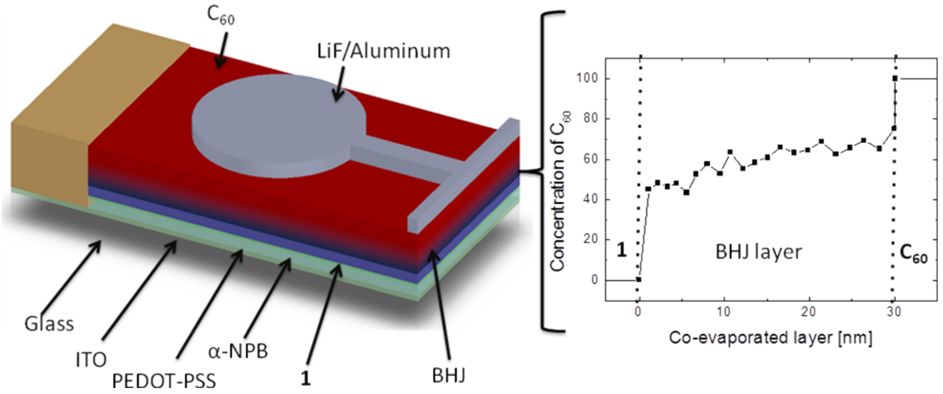

Fig. S14 Schematic representation of the BHJ cell and profile of C$_{60}$ concentration in the active layer.

The EQE action spectrum of the best bulk heterojunction solar cell has been measured with a homemade system using optical filters (from 400 nm to 900 nm) and a calibrated photodiode (Fig. S15). From this result, we have extracted a current density of 9.1 mA/cm^2 (J_{sc}) at 0 V in agreement with *J vs V* measurements under illumination.

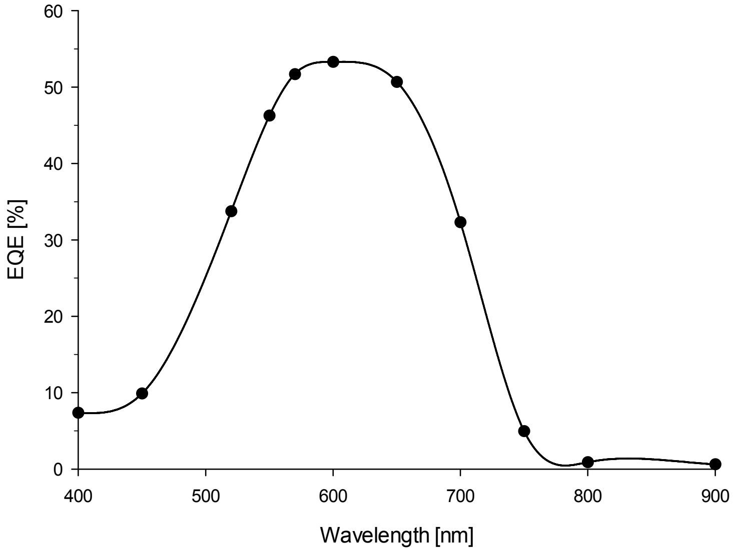

Fig. S15 Plot of the EQE action spectrum of the best BHJ solar cell based on **1** recorded from 400 nm to 900 nm.

5. Mobility measurements (performed at LPICM-Polytechnique)

To estimate the hole-transport properties of molecular films of **1**, we fabricated and analyzed a hole-injection diode. Fig. S16 (top) shows the device structure containing a 100 nm layer of **1** obtained by evaporation and the current-density-voltage (*J-V*) characteristics of such a device. It is observed that the current is higher when the PEDOT:PSS side is more positively biased than the Au electrode, which is mainly attributed to the difference in the injection barriers. In such a situation, an energetic asymmetry leads to a formation of non-zero internal field at equilibrium, so that the measured *J-V* characteristics should be corrected by the corresponding built-in potential (V_{bi}). Fig. S16 (bottom) shows that, by assuming V_{bi} of 0.3 V, the current density injected from the PEDOT:PSS follows a quadratic dependence on V-V_{bi} at high voltage, indicating space-charge-limited conduction (SCLC). We can fit the experimental data in this regime to the Mott-Gurney law including the voltage correction term as

$$J = \frac{9}{8}\mu\varepsilon_s \frac{(V - V_{bi})^2}{L^3}, \quad (1)$$

where μ is the charge-carrier mobility, ε_s is the semiconductor permittivity, and L is the semiconductor thickness. By assuming a dielectric constant of 3, the extracted hole mobility μ of **1** is 3.4×10^{-5} cm^2/Vs, which is comparable to reported SCLC mobility values found on many small molecular donors in a diode configuration.

The same experiments have been carried out also with compound reference **2** affording a hole mobility value of 2×10^{-6} cm^2/Vs.

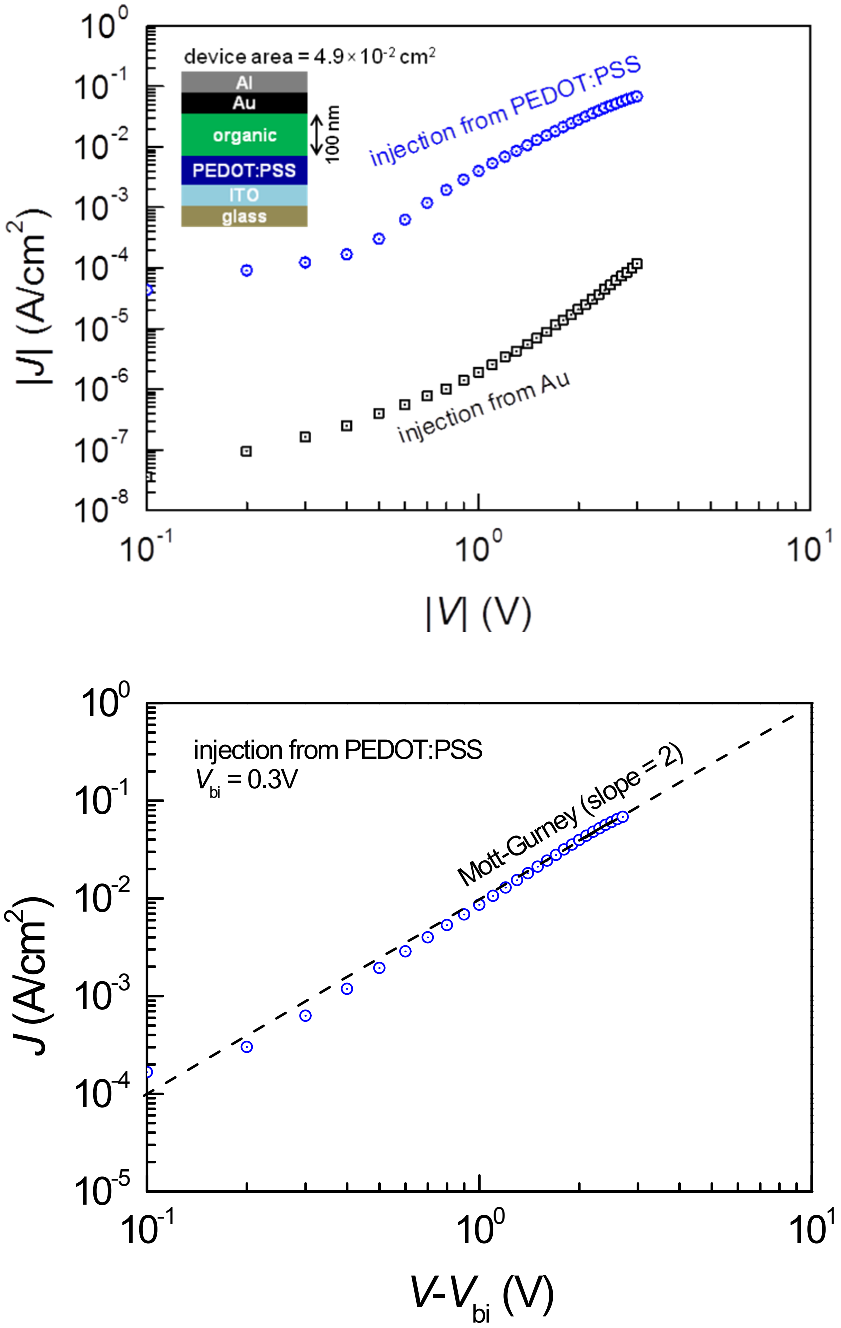

Fig. S16 Top: current density–voltage characteristics of a hole-only diode based on **1**. The inset is the device structure. Bottom: current density–voltage curve for the injection from PEDOT:PSS corrected by the built-in potential (V_{bi}). The mobility is extracted by fitting the measured data to the Mott–Gurney law in the high-voltage region.